A POSSIBLE MODIFICATION OF CERAMIC CHAMBERS IN THE INJECTION AREA AT THE RCS IN J-PARC

Y. Shobuda*, J. Kamiya, T. Takayanagi, JAEA/J-PARC, Ibaraki, Japan
K. Horino, T. Ueno, T. Yanagibashi, NAT, Ibaraki, Japan
H. Kotoku, ULVAC, Kanagawa, Japan

Abstract

At the injection area of the RCS in J-PARC, the interaction between the copper stripes (RF-shields) on the ceramic chambers and the external magnetic fields modulates the magnetic fields in the chamber, causing beam losses for a special tune. A ceramic chamber spirally covered by the stripes is a candidate to mitigate the modulations. In this report, we numerically and experimentally investigate how the interaction is suppressed, while sustaining the beam impedance enhancement within tolerable at the RCS.

INTRODUCTION

The RCS at J-PARC [1] has demonstrated a 1-MW-eq. beam [2, 3] by accumulating H^- beams from LINAC into two bunches at the RCS. When the two bunched beams, each containing 4.15×10^{13} particles per bunch, are accelerated from 400 MeV to 3 GeV at a repetition rate of 25 Hz, the 1-MW beam can be performed at the RCS.

To suppress the eddy current on metal chambers caused by such rapidly changing magnets during the acceleration period, we adopt ceramic chambers covered over copper stripes whose one ends are terminated by capacitors [4]. The capacitance is typically determined by the low impedance for the circulating beam and the high impedance for the current with the frequency, characterized by the ramping time (20 ms) [5].

From a beam instability point of view [6–11], the chambers are not harmful, except the injection period when 'four dipole magnets' with different polarities (+–+) at the injection area specifically excite the trapezoid field pattern [5, 12], accumulating the LINAC beams. Since the copper stripes and flanges create an inductance, the inductance in combination with the capacitors makes LCR electric circuit on the chamber, which excites the induced current on the copper stripes during the injection period. The field modulation excited the current could cause beam losses for the circulating beams at the RCS [2, 12].

It is noticeable that the effect of the field modulation on the circulating beams can be canceled out after the beams pass through four dipole magnets, only when all dipole magnets including the chambers are perfectly identical. Hence, all dipole magnets are designed to be as identical as possible at the present RCS from both mechanical and electrical points of view. Still, the identity of the chambers is imperfect in reality, because of the distinct of respective chambers (for example, the chamber embedding the charge-exchange

foil holds a slot through which the foil is inserted into the chamber). Such imperfections among four chambers cause significant beam losses for a specified tune [2, 12].

To enhance the machine tunability, let us consider a ceramic chamber over which RF-shields spirally [13] cover. In this case, the induced voltage excited from the external magnetic flux on the RF-shields can be canceled out within each chamber in the lowest-order approximation, though we need to investigate to what degree the coupling impedance [6] of the ceramic chambers is enhanced, compared to that of conventional ones.

THE EFFECT OF THE MAGNETIC FLUX

Let us investigate the effect of the external magnetic flux on the spiral chamber by measurements and simulations. To demonstrate the proof of principle, we fabricate (type-1) a $L = 1060$ mm long rectangular chamber (($2a_H = 405$ mm) × ($2a_V = 265$ mm)) with $W = 5$ mm thickness, made of 'Bakelite' with relative dielectric constant $\epsilon' \simeq 5$, instead of ceramic with $\epsilon' = 11$. The left picture of Fig. 1 shows a schematic picture of the chamber over which 66 number of RF-shields cover spirally. One ends of the stripes are terminated by the capacitor with its electric impedance Z.
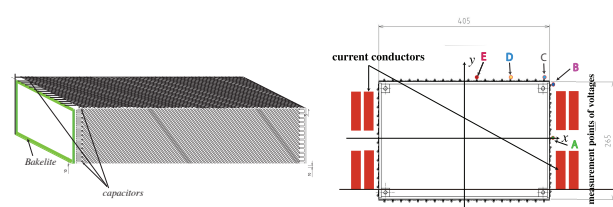

Figure 1: Spiral chamber (left) and the setup to measure induced voltages due to the magnetic flux (right).

To determine the input parameters for simulations to be compared with the measurements, let us measure the impedance Z as a function of frequency f. We prepared two electric elements (1) a capacitor embedded in a copper stripe and (2) the other copper stripe of the same length (see the left of Fig. 2). The measurements were done by LCR-meter [14]. The frequency dependence of the impedance Z for the capacitor was obtained by subtracting the result of (2) from the result of (1). The red circle and the blue square represent the real and the imaginary parts of Z. Based on the measured

data, the impedance Z is parameterized as

$$Z = \frac{1}{j\omega C + \frac{1}{R_p}},\qquad(1)$$

(the dot and solid lines in Fig. 2), where j is imaginary unit, ω is angular frequency, $C = 94.6$ nF and $R_p = 922$ Ω.
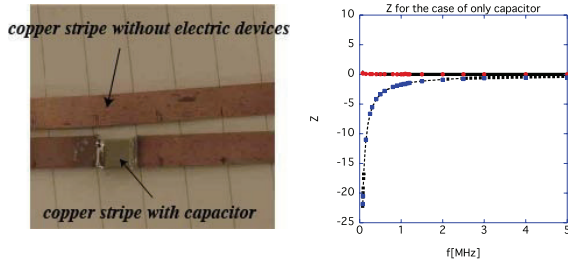

Figure 2: Two devices (left), and Z for the capacitor (right).

The right picture of Fig.1 shows the measurement setup, where the chamber is placed inside the dipole magnet embedding the current conductors, which flow the trapezoid form current in the time domain (In this picture, the current conductor has bundled four turns inside the magnet.).

Given a conductor current (the current uprises to 4×10 kA during 800 μs), we observe the induced voltages on the capacitors placed at positions A, B, C, D, and E in Fig. 1. The measurements and the simulations by using CST [15] are shown in the left and the right figures in Fig. 3, respectively. The green, purple, black, blue, and red lines correspond to the results observed at A, B, C, D, E in Fig. 1, respectively. The min-window in the left picture of Fig. 3 shows the measurements for a conventional case that the RF-shields are uniformly placed on the chamber in the longitudinal direction, for reference. The simulation results fairly explain the amounts of amplitudes in the measurements. Though we can still see the current oscillation on the RF-shields because of the defects of the symmetry in the azimuthal direction, the measurements demonstrate that the spiral RF-shields can suppress the oscillation amplitudes compared to those on the conventional RF-shields.
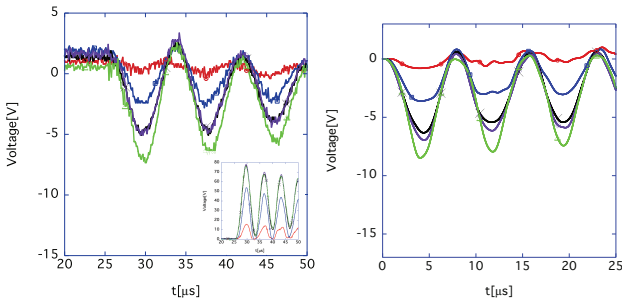

Figure 3: Measured voltages (left) and simulated ones (right) on the capacitors.

Following the agreement of the measurements and simulations, we simulate (type-2) the $L = 1340$ mm long 'ceramic' chamber $((a_H = 479$ mm$)\times(a_V = 289$ mm$))$

with $W = 9$ mm thickness, whose surface is covered over 142 number of copper stripes. Besides, we assume the other chamber holding a narrow slot $((l = 268$ mm$)\times(w = 30$ mm$))$, perpendicular to the beam direction. The important point to suppress the induced voltage is securing the current path which flows spirally along with the chamber, so that the slot must be enclosed by conductive metal which is attached with the ends of all RF-shields crossing the slot.

Now, let us see this slot effect on the induced current so that we compare the spiral RF-shields without the slot to those with the slot. The results are shown in Fig. 4, where the conductor current uprises to 44.2 kA during 400 μs. As expected, the oscillation amplitudes with the slot (left) are enhanced due to the imperfect spiral structure caused by the slot. But, it is still tolerable compared to the oscillation amplitudes observed in the conventional RF-shielded chambers (see mini-window in Fig. 3).
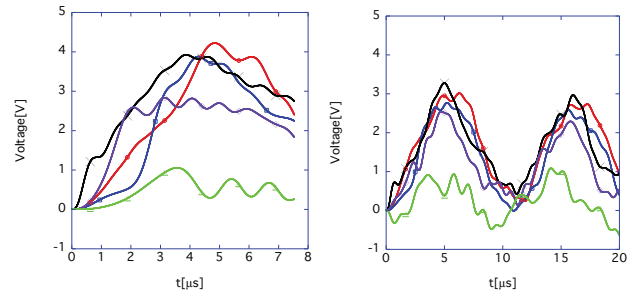

Figure 4: Simulations of induced voltages on the capacitors for the spiral chamber with (left) and without a slot (right).

BEAM IMPEDANCE ENHANCEMENTS

Now, let us investigate the beam impedances, and see to what degree the impedance of the spiral chamber with the slot is enhanced compared to that of the conventional one.

For a cylindrical ceramic chamber simply covered over perfectly conductive wall, we can estimate the longitudinal Z_L and horizontal Z_x impedances analytically, which are given by [16–18]

$$Z_L[\Omega] \simeq j\frac{Z_0 L(\epsilon' - 1)\frac{\omega}{c}\log[\frac{a}{a-w}]}{2\pi\epsilon'},\qquad(2)$$

$$Z_x[\Omega/\text{m}] \simeq j\frac{Z_0 L(\epsilon' - 1)\log[\frac{a}{a-w}]}{\pi a^2\epsilon'},\qquad(3)$$

where $Z_0 = 120\pi$ [Ω] is impedance of free space, c is light velocity, a is the radius of the chamber. And, the impedances of a narrow slot $(l \times w)$ perpendicular to the longitudinal direction can be estimated as [19, 20]

$$Z_L[\Omega] \simeq j\frac{0.132 Z_0 \omega l^3}{4\pi^2 a^2 c\log[1 + \frac{0.66l}{w}]},\qquad(4)$$

$$Z_x[\Omega/\text{m}] \simeq j\frac{0.132 Z_0 l^3}{\pi^2 a^4 \log[1 + \frac{0.66l}{w}]},\qquad(5)$$

12th Int. Particle Acc. Conf.
IPAC2021, Campinas, SP, Brazil
JACoW Publishing
ISBN: 978-3-95450-214-1
ISSN: 2673-5490
doi:10.18429/JACoW-IPAC2021-WEPAB245

where we assume that the magnetic polarities dominate compared to the electric ones in the slot perpendicular to the beam direction. Here, if we evaluate a as the average of a_H and a_V, Eqs. (2) and (3) are $Z_L \sim j0.0323[\Omega/\text{MHz}] \cdot f[\text{MHz}]$, and $Z_x \sim j110[\Omega/\text{m}]$ for (type-1) chamber, respectively, while Eqs.(2), (3), (4) and (5) are $Z_L \sim j0.0735[\Omega/\text{MHz}] \cdot f[\text{MHz}]$, $Z_x \sim j190[\Omega/\text{m}]$, $Z_L \sim j0.00714[\Omega/\text{MHz}] \cdot f[\text{MHz}]$ and $Z_x \sim j37[\Omega/\text{m}]$ for (type-2) chamber with the slot, respectively. The contribution from the slot to the total impedances of the RF-shielded chamber is smaller in the order of magnitude.

Now, let us simulate the impedance of the conventional ceramic chamber with capacitors, where RF-shields are uniformly placed in the longitudinal direction. The left and right pictures in Fig. 5 show the longitudinal and horizontal impedances without the slot, respectively. The red and the blue lines denote the real and imaginary parts of the impedance, respectively. The analytical estimation for the (type-2) chamber fairly evaluates the simulations except for the enhancement at low frequency due to the capacitors.

Figure 6 shows the simulation result of the longitudinal (left) and the horizontal (right) impedances for the spiral chamber with (solid lines) and without the slot (dashed lines), where the red/black and the blue/green lines denote the real and imaginary parts of the impedances, respectively. Compared to the conventional results in Fig. 5, the inductive (imaginary) parts are enhanced for both longitudinal and horizontal impedances, because of the spiral structure of the RF-shields. On the other hand, since the radiation effects are negligible at low frequency, the difference between the real parts of the impedances cannot be identified for both
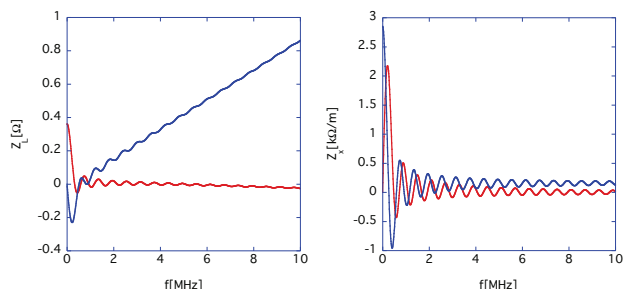
cases. As the analytical results suggested, the simulations demonstrate that the slot does not affect the impedance enhancements significantly.

To demonstrate the impedance enhancement, let us measure the electric impedance Z_{ele} of (type-1) 'Bakelite' chamber with spiral RF-shields and of with uniform RF-shields, by using LCR-meter [14]. A schematic picture of the measurement setup is shown in Fig. 7. For the respective chambers, Z_{ele} is measured as in the left picture, and the impedances of the reference chamber are measured as in the right picture after the respective chambers are covered over Aluminum.

Figure 7: Measurement setup for Z_{ele}.

The measurements subtracting the reference impedance are illustrated in the left figure of Fig. 8. The simulations are shown in the right picture of Fig. 8. The solid and the dashed lines show the results of the spiral and those of the conventional chambers, respectively. The red/black and blue/green lines show the real and imaginary parts of the impedance, respectively. The simulations fairly explain the measurements for the conventional chamber, while we can see a discrepancy for the spiral chambers at high frequency. Note that the measurements above 6 MHz are less reliable, because of the negativity of the red line. Though the electric impedance, which is not obtained by a standard single wire method [19], is not identical to the longitudinal beam impedance, we can indirectly confirm the impedance enhancement by the measurements.

Figure 5: Simulations of Z_L (left) and Z_x (right) for the conventional chamber without the slot.

Figure 8: Measured Z_{ele} (left) and simulated one (right).

SUMMARY

The ceramic chamber spirally covered over RF-shields can mitigate the field modulation at the injection area of J-PARC RCS. On the other hand, the beam impedance is slightly enhanced, compared to the impedance of the present RF-shielded ceramic chamber.
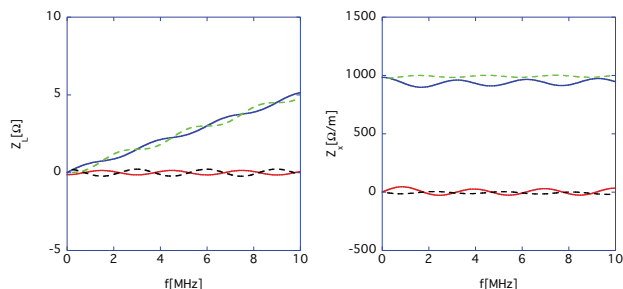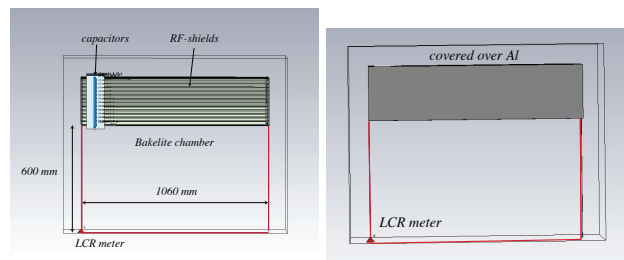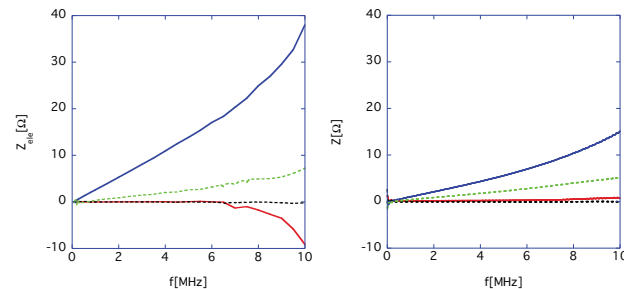

Figure 6: Simulations of Z_L (left) and Z_x (right) for the spiral chamber with (solid) and without the slot (dashed).

REFERENCES

[1] Japan Proton Accelerator Research Complex, http://j-parc.jp/index-e.html

[2] H. Hotchi *et al.*, "Achievement of low-loss 1-MW beam operation in the 3-GeV rapid cycling synchrotron of the Japan Proton Accelerator Research Complex", *Physical Review Accelerators and Beams*, vol. 20, p. 060402, Jun. 2017. doi:10.1103/PhysRevAccelBeams.20.060402

[3] H. Hotchi *et al.*, "Realizing a High-Intensity Low-Emittance Beam in the J-PARC 3-GeV RCS", in *Proc. 8th Int. Particle Accelerator Conf. (IPAC'17)*, Copenhagen, Denmark, May 2017, pp. 2470–2473. doi:10.18429/JACoW-IPAC2017-WEOAA3

[4] M. Kinsho *et al.*, "Development of alumina ceramics vacuum duct for the 3 GeV-RCS of the J-PARC project", *Vacuum*, vol. 73, pp. 187-193, Mar. 2004. doi:10.1016/j.vacuum.2003.12.043

[5] Y. Shobuda, Y. Irie, and S. Igarashi, "Analytical method for the evaluation of field modulation inside the rf-shielded chamber with a time-dependent dipole magnetic field", *Physical Review Special Topics - Accelerators and Beams*, vol. 12, p. 032401, Mar. 2009. doi:10.1103/PhysRevSTAB.12.032401

[6] A. W. Chao, *Physics of Collective Beam Instabilities in High Energy Accelerators*, New York, USA: Wiley, 1993.

[7] Y. Shobuda *et al.*, "Theoretical elucidation of space charge effects on the coupled-bunch instability at the 3 GeV rapid cycling synchrotron at the Japan Proton Accelerator Research Complex", in *Progress of Theoretical and Experimental Physics*, vol. 2017, no. 1, p. 013G01, Jan. 2017. doi:10.1093/ptep/ptw169

[8] Y. Shobuda *et al.*, "Coupled Bunch Instability and Its Cure at J-PARC RCS", in *Proc. 8th Int. Particle Accelerator Conf. (IPAC'17)*, Copenhagen, Denmark, May 2017, pp. 2946–2949. doi:10.18429/JACoW-IPAC2017-WEPIK014

[9] P. K. Saha *et al.*, "Simulation, measurement, and mitigation of beam instability caused by the kicker impedance in the 3-GeV rapid cycling synchrotron at the Japan Proton Accelerator Research Complex", *Physical Review Accelerators and Beams*, vol. 21, p. 024203, Feb. 2018. doi:10.1103/PhysRevAccelBeams.21.024203

[10] Y. Shobuda *et al.*, "Reducing the beam impedance of the kicker at the 3-GeV rapid cycling synchrotron of the Japan Proton Accelerator Research Complex", *Physical Review Accelerators and Beams*, vol. 21, no. 6, p. 061003, Jun. 2018. doi:10.1103/PhysRevAccelBeams.21.061003

[11] Y. Shobuda *et al.*, "Measurement scheme of kicker impedances via beam-induced voltages of coaxial cables", *Nuclear Instruments and Methods in Physics Research Section A: Accelerators, Spectrometers, Detectors and Associated Equipment*, vol. 713, pp. 52–70, Jun. 2013. doi:10.1016/j.nima.2013.02.037

[12] Y. Shobuda and Y. Irie, "Analytical Estimation of the Field Modulation during the Injection Period of the 3GeV RCS in J-PARC", in *Proc. of the 2nd Int. Symposium on Science at J-PARC — Unlocking the Mysteries of Life, Matter and the Universe*, Tsukuba, Japan, Jul. 2014, vol. 8, p. 012003. doi:10.7566/JPSCP.8.012003

[13] A. Chmielinska and M. J. Barnes, "New Spiral Beam Screen Design for the FCC-hh Injection Kicker Magnet", in *Proc. 10th Int. Particle Accelerator Conf. (IPAC'19)*, Melbourne, Australia, May 2019, pp. 270–273. doi:10.18429/JACoW-IPAC2019-MOPGW074

[14] Agilent Technologies, Now, Keysight Technologies, https://www.keysight.com/jp/ja/home.html

[15] CST Studio Suite, https://www.3ds.com/products-services/simulia/products/cst-studio-suite/?utm_source=cst.com&utm_medium=301&utm_campaign=cst

[16] Y. Shobuda, Y. H. Chin, K. Ohmi, and T. Toyama, "The Impedance of the Ceramic Chamber in J-PARC", in *Proc. 21st Particle Accelerator Conf. (PAC'05)*, Knoxville, TN, USA, May 2005, paper MPPP025, pp. 1898–1900.

[17] Y. H. Chin, S. Lee, Y. Shobuda, K. Takata, T. Toyama, and H. Tsutsui, "Impedance and radiation generated by a ceramic chamber with RF shields and TiN coating", in *Proc. 39th ICFA Advanced Beam Dynamics Workshop on High-Intensity and High-Brightness Hadron Beams (HB'06)*, Tsukuba, Japan, May-Jun. 2006, paper TUBX01, pp. 125-127.

[18] Y. Shobuda and M. Kinsho, "Reproduction of Ceramic Chamber Impedances with Electric and Magnetic Polarities of the Ceramics", in *Proc. 3rd Int. Particle Accelerator Conf. (IPAC'12)*, New Orleans, LA, USA, May 2012, paper WEPPR056, pp. 3051–3053.

[19] A. W. Chao and M. Tigner, *Handbook of Accelerator Physics and Engineering*, Singapore: World Scientific Publishing, 1999.

[20] N. A. McDonald, "Simple approximations for the longitudinal magnetic polarizabilities of some small apertures", *IEEE Transactions on Microwave Theory and Techniques*, vol. 36, no. 7, pp. 1141–1144, Jul. 1988. doi:10.1109/22.3648